# *In situ* HREM irradiation study of point-defect clustering in MBE-grown strained $Si_{1-x}Ge_x/(001)Si$ structures

L. Fedina,* O. I. Lebedev,† G. Van Tendeloo, and J. Van Landuyt‡
*EMAT, RUCA, Groenenborgerlaan 171, B-2020 Antwerpen, Belgium*

O. A. Mironov§ and E. H. C. Parker
*Department of Physics, University of Warwick, Coventry CV4 7AL, United Kingdom*
(Received 27 July 1999)

We present a detailed analysis of the point-defect clustering in strained $Si/Si_{1-x}Ge_x/(001)Si$ structures, including the interaction of the point defects with the strained interfaces and the sample surface during 400 kV electron irradiation at room temperature. Point-defect cluster formation is very sensitive to the type and magnitude of the strain in the Si and $Si_{1-x}Ge_x$ layers. A small compressive strain ($-0.3\%$) in the SiGe alloy causes an aggregation of vacancies in the form of metastable [110]-oriented chains. They are located on {113} planes and further recombine with interstitials. Tensile strain in the Si layer causes an aggregation of interstitial atoms in the forms of additional [110] rows which are inserted on {113} planes with [001]-split configurations. The chainlike configurations are characterized by a large outward lattice relaxation for interstitial rows ($0.13 \pm 0.01$ nm) and a very small inward relaxation for vacancy chains ($0.02 \pm 0.01$ nm). A compressive strain higher than $-0.5\%$ strongly decreases point-defect generation inside the strained SiGe alloy due to the large positive value of the formation volume of a Frenkel pair. This leads to the suppression of point-defect clustering in a strained SiGe alloy so that SiGe relaxes via a diffusion of vacancies from the Si layer, giving rise to an intermixing at the Si/SiGe interface. In material with a 0.9% misfit a strongly increased flow of vacancies from the Si layer to the SiGe layer and an increased biaxial strain in SiGe both promote the preferential aggregation of vacancies in the (001) plane, which relaxes to form intrinsic 60° dislocation loops.

## I. INTRODUCTION

Strained SiGe/Si structures are an essential component of many advanced Si-based devices; however, the mechanism of strained-layer relaxation by means of point-defect interaction, for instance, during thermal annealing, and the effect of strain on point-defect clustering are still poorly understood. In particular, Iyer and LeGoues have reported an enhanced Ge-Si interdiffusion which is ''frozen'' by the formation of a high density of dislocations.[1] This observation was attributed to strain-assisted diffusion, based on the thermodynamic analysis of spinodal decomposition by Cahn and Hilliard,[2] but no specific physical mechanism for this phenomenon has so far been proposed. Additionally, the effect of biaxial strain in strain-assisted diffusion in SiGe layers is controversial at present, the reported strain effect varying from huge to barely discernable.[3–8] A first step to the understanding of strain-assisted diffusion was made by total-energy calculations.[9] Antonelli and Bernholc computed the formation energies for self-interstitials ($\Delta E_{fI}$) and vacancies ($\Delta E_{fV}$) in Si as a function of hydrostatic pressure. A linear increase in $\Delta E_{fI}$ and a decrease in $\Delta E_{fV}$ are found with increasing pressure, corresponding to an outward relaxation of the lattice around the interstitial atom, and an inward relaxation of the vacancy. Recently, a thermodynamic formalism was developed for illuminating the predominant point-defect mechanism of self- and impurity diffusion in silicon, which was also used to provide a rigorous basis for the point-defect-based interpretation of diffusion experiments in biaxially strained epitaxial layers in the SiGe system.[10] Quantitative agreement between the calculated atomistic parameters for the vacancy mechanism and biaxial strain experiment has been found for the case of Sb diffusion and only qualitative agreement for an interstitial-based mechanism has been found for the case of boron diffusion. It was concluded that critical experiments and calculations for the determination of key parameters (activation volumes) of the interstitial-based mechanism are needed.

We will attempt to show in the present paper that the relaxation volume of a self-interstitial atom in Si ($V_I^{\mathrm{rel}}$) can be determined from the analysis of experimental high-resolution electron microscopy (HREM) images of linear clusters of interstitial atoms. The value of $V_I^{\mathrm{rel}} = 0.94\Omega$ agrees well with that obtained from tight-binding molecular dynamics studies ($0.90\Omega$).[11] Here $\Omega = 0.020\ \mathrm{nm}^3$ is the atomic volume per silicon atom at equilibrium density. However, to elucidate clustering of point defects in a strained heterostructure both the relaxation volumes for an interstitial atom and for a vacancy ($V_V^{\mathrm{rel}}$) are needed because their sum determines the formation volume of a separated Frenkel pair ($V_F^f$); in other words, the possibility of Frenkel pair separation. The reported values of $V_V^{\mathrm{rel}}$ vary in a range between $-0.25\Omega$ and $-0.97\Omega$,[9,11,12] so that $V_F^f$ is changed from a large positive amount ($0.65\Omega$) to a negative one ($-0.07\Omega$) and consistent prediction of Frenkel pair separation in strained lattices becomes impossible. The very small inward relaxation (within $0.02 \pm 0.01$ nm) around the chainlike configuration of vacancies, which we report here, strongly suggests that $V_V^{\mathrm{rel}}$ is rather small and cannot compensate $V_I^{\mathrm{rel}}$ as predicted in Ref. 11. The difference between

 

$V_V^{rel}$ and $V_I^{rel}$ gives us also a chance to understand why the interaction coefficient of vacancies with the real Si surface (or with surfaces capped by thin $SiO_2$ and $Si_3N_4$ films) is much larger than that for self-interstitials (up to two orders of magnitude). This important conclusion was made on the basis of a detailed investigation of the aggregation of self-interstitial atoms in Si and Ge by *in situ* irradiation experiments in a high-voltage electron microscope (HVEM) over a wide temperature range between 20 and 1150 °C.[13] The larger vacancy capture coefficient of the surface results in an interstitial supersaturation close to the Si sample surface during irradiation, even at room temperature.[14] But no clusters of point defects are created in unstrained and low-doped Si or Ge crystals covered with native oxide films (1 nm) until the thickness of the irradiated specimen reaches 200–300 nm.[13] Whereas, inside the bulk of Si, the recombination of point defects dominates and no clusters are formed, interstitial clusters known as {113} defects immediately form near the surface. Their nucleation is caused by multiatom interaction since the chemical stresses $E_{ch}=kT\ln(C_{i_i}/C_{i0})$ are much larger than the interaction energy of point defects with elastic stresses $E_{el}=\frac{4}{3}(\pi\Delta a/a)\Omega\sigma_{ii}$.[13] Here $C_i$ and $C_{i0}$ are the concentrations of interstitials in the irradiated crystal and in thermal equilibrium, respectively, $\sigma_{ii}$ are the elements of the elastic stress tensor, and $\Delta a/a$ is the deformation of the crystalline lattice by a single interstitial atom. As a result, the effect of elastic stress on the nucleation of interstitial clusters was concluded to be negligible. However, this effect can be observed in very thin Si specimens, where quasistationary concentrations of point defects during irradiation are smaller than in thick specimens. Recently, clustering of intrinsic point defects at room temperature in thin Si specimens covered with $Si_3N_4$ films was shown to be much more complex than earlier assumed and included a combined aggregation of vacancies and interstitial atoms on {111} and {113} habit planes.[14–16] The driving force proposed for this process is either a compensation of large strains caused by initial clustering of vacancies on {111} or a slow recombination of point defects in extended shape on {113}.[17] In general, however, the role of strain in point-defect clustering is not yet clear.

Our previous HREM irradiation experiments with strained Si/SiGe/(100)Si structures showed that some new information concerning point-defect clustering depending on the type and magnitude of local strains in Si and SiGe layers could be obtained.[18] The present paper is a detailed analysis of the point-defect clustering in a strained SiGe system, including the interaction of point defects with the strained interfaces and the surface of the specimen during electron irradiation in a HREM.

## II. EXPERIMENTAL DETAILS

The samples are *p*-type boron-modulated-doped and coherently strained $Si/Si_{1-x}Ge_x/(001)Si$ heterostructures with $X=0.08$ and 0.13,[19,20] and undoped five-period multiple quantum wells (MQWs) with $X=0.22$,[21–23] and with a thickness of the SiGe layers of 35, 40, and 3–6 nm, respectively. They were grown using solid-source molecular beam epitaxy (MBE) VG Semicon V90S equipment.[19,20] The concentration of Ge in fully strained SiGe layers has been determined by high-resolution x-ray diffraction, ULE secondary-ion mass spectroscopy, Raman, Rutherford backscattering, and conventional XTEM analysis.[21–23]

(110) cross-section specimens for HREM were presented by standard Ar ion milling using a low voltage and a low ion-beam inclination, which avoids damage in the sample. *In situ* HREM experiments were carried out at room temperature in a JEOL-4000EX microscope operating at 400 keV and allowing a point resolution of 0.17 nm. The energy of the electron beam used in our experiment exceeds the threshold of 200 keV for generation of Frenkel pairs in Si crystals, but not in Ge (470 keV).[24] The flux of electrons during the HREM irradiation experiments was estimated to be close to $10^{20}$ electrons/cm$^2$ s (see also Ref. 25). According to the results presented in Ref. 13, an additional specimen heating upon 400 keV irradiation does not exceed 50 °C. Atomic models of the point-defect aggregates have been obtained by comparing experimental HREM images with simulated images using the MAC TEMPAS software.

## III. RESULTS

It is known that the atomic scale study of very small clusters by HREM methods is not straightforward. Detailed and correct information can only be obtained for extended one- (1D) or two-dimensional (2D) clusters having a periodic structure along the electron beam (in the present case the [110] direction). It will be further demonstrated that the size of the defect along this direction has to be at least 60% of the foil thickness. All the HREM images presented in this study were recorded at defocus values between $-20$ and $-55$ nm. According to the image simulations bright dots then correspond to the channels in the Si structure in a range of foil thickness between 1 and 22 nm at the defocus of $-20$ nm and at least between 1 and 6 nm at the defocus of $-55$ nm. In this case dark columns between white dots in the HREM image correspond to the atomic chains in the [110] direction.

According to Vegard's law, in the absence of relaxation via dislocations, the strain $s$ is related to the Ge composition $x$ by the relation $s=(1-a_{Ge}/a_{Si})x=-0.042x$.[5] The minus sign indicates a compressive strain. Assuming no contribution from the top and bottom free surfaces on the strain relaxation during HREM specimen preparation, the corresponding strains in $Si/Si_{1-x}Ge_x/(001)Si$ structures used in our experiments were about 0.3, 0.5, and 0.9 %.

### A. Low-strain $Si_{1-x}Ge_x$ system with $x=0.08$ and $s=0.3\%$

Figures 1(a), 1(b), and 1(c) show a sequence of lower-magnification (110) cross-section HREM images of a strained $Si/Si_{1-x}Ge_x/(100)Si$ heterostructures ($x=0.08$, $s=0.3\%$, SiGe layer width 35 nm) in the initial stage and at further stages of irradiation. Since the concentration of Ge atoms in the alloy is small, the position of the SiGe layer is hardly visible in the HREM mode in Fig. 1(a). However, this layer is easy to locate using conventional two-beam diffraction conditions. From Fig. 1(a) it is clear that the irradiated area is defect-free in the initial stage of irradiation. After about 10 minutes of irradiation small clusters of point defects are created, and the position of the SiGe layer becomes visible due to the formation of defects inside this layer and close to the interfaces [Fig. 1(b)]. Few defects are created in

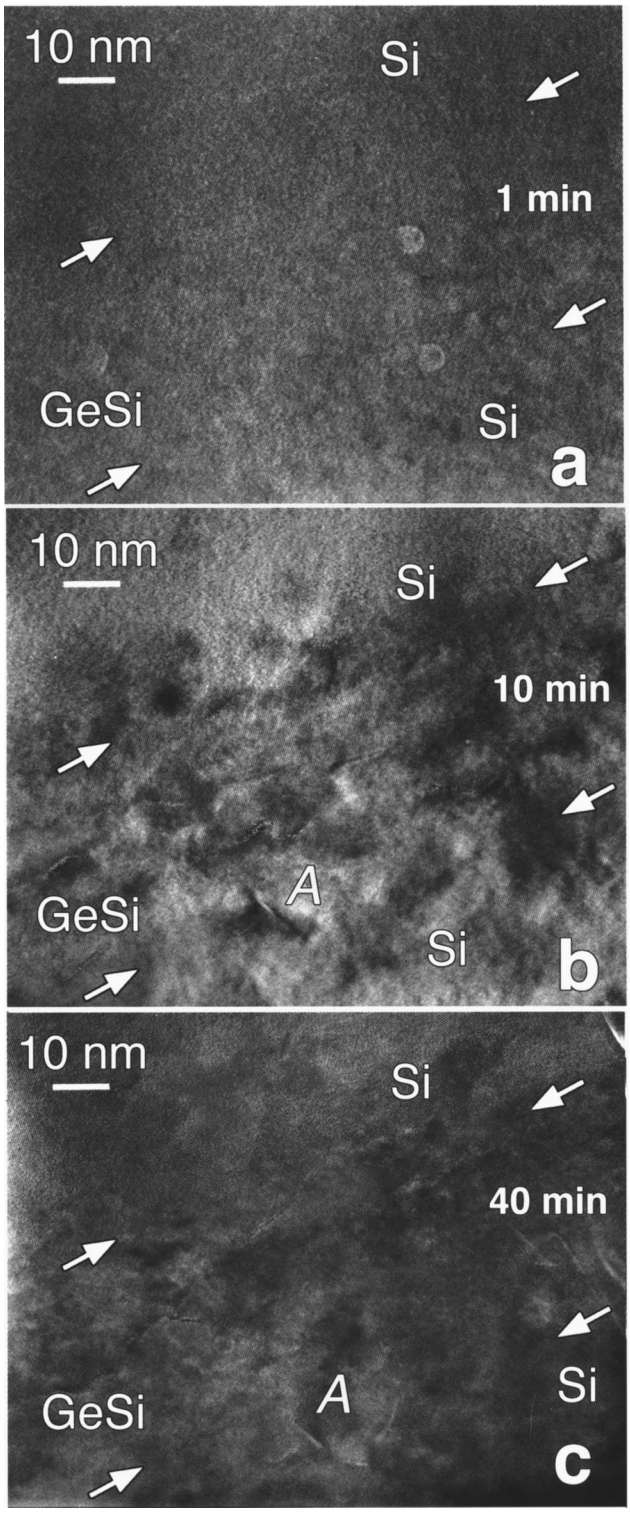


FIG. 1. [110] HREM images of point-defect clusters introduced in a strained Si/SiGe/(001)Si heterostructure with 0.3% misfit during *in situ* electron irradiation in a 400 kV microscope at room temperature. The same irradiated area is shown as a function of time: (a) 1 min; (b) 10 min; (c) 40 min. White arrows roughly indicate the position of the SiGe/Si interfaces within the irradiated area.

the Si layer at a large distance ($>5$ nm) from the SiGe/Si interfaces during irradiation [Fig. 1(c)]. At the same time in the SiGe layer the defect density first increases (up to $10^{12}$ cm$^2$) and then strongly decreases.

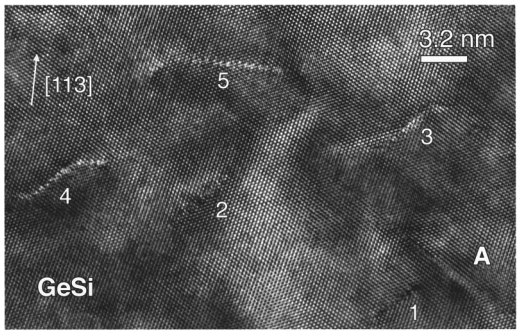


FIG. 2. An enlarged HREM image of the point-defect clusters created within the 0.3% misfit SiGe after 25 min of irradiation. The defect marked as *A* is the same defect as shown in Fig. 1.

An enlarged HREM image of clusters created inside the SiGe layer at a further stage comparable to Fig. 1(b) is shown in Fig. 2. Most of the defects are located on {113} habit planes (e.g., those marked 1, 2, 3, 4, and 5) and few are on {111} (marked by *A*). The defect on {111} is a small Frank dislocation loop, visibly characterized as a vacancy loop by the distortion of the {111} planes parallel to the defect plane. Defects lying on {113} planes are much more complex because usually there is no visible displacement of the atomic columns around such defects. However in some images, for instance, at the defect number 5, a very small vacancy sign distortion of the {113} planes parallel to the defect plane is visible. This defect is enlarged in Fig. 3(a) with an atomic model superimposed on the experimental HREM image in Fig. 3(b). The model consists of a sequence of eight- and ten-membered atomic rings located close to the {113} habit plane. Each of the eight-membered rings encloses three white dots. Two of them, which are located on the left and on the right from the middle one, correspond to two channels in SiGe. The middle one is formed at the position of the atomic column, as is clearly seen from Fig. 3(b). We assume that this white dot corresponds to a vacancy chain caused by aggregation of vacancies in the [110] direction along the incident electron beam.

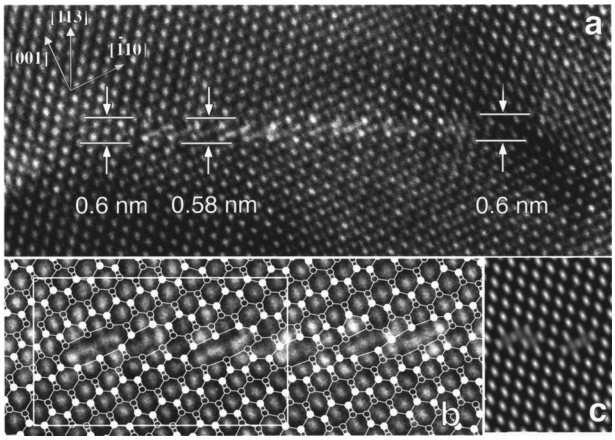


FIG. 3. (a) [110] HREM image of a {113} defect in strained SiGe with 0.3% misfit. The small distortion of the {113} planes parallel to the defect plane is shown by white lines. (b) An atomic model of the {113} defect is superimposed on the image. (c) A simulated HREM image of a {113} defect based on the unit cell indicated in (b) by the white rectangle.

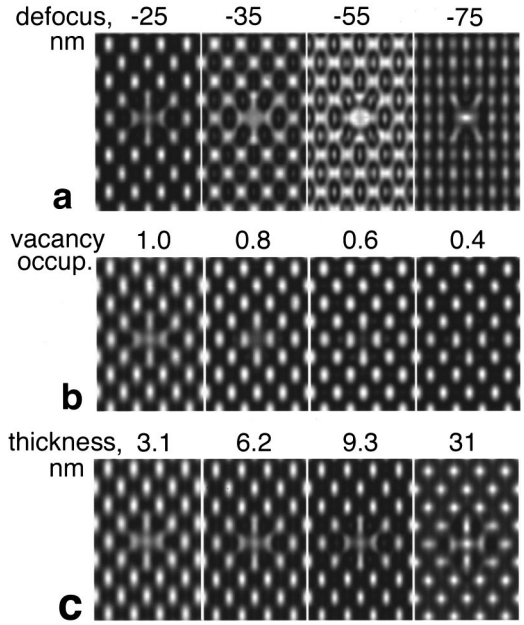


FIG. 4. (a) Simulated HREM images of the single-vacancy chain as a function of defocus for a fixed crystal thickness of 9.3 nm. (b) Simulated image as a function of the vacancy content in the atomic chain. Focus value and crystal thickness are $-25$ nm and 3.1 nm, respectively. (c) Crystal thickness dependence of the HREM image for a fixed defocus value of $-25$ nm.

Ten-membered rings enclose two nearest-neighbor atomic columns where vacancies aggregate and become double-vacancy chains. The arrangement of the vacancies along the [110] direction cannot be deduced from the HREM image. However, it is sensitive to the vacancies in the atomic chain as we will show later by image simulation. In our tentative model of a vacancy type {113} defect [Fig. 3(b)] consisting of vacancy chains, vacancies in the [110] direction are considered as a continuous vacancy chain in which no dangling bonds are involved along the chain (excluding, of course, two dangling bonds at the edges of the chain). The model of a continuous vacancy chain as a simple arrangement for minimizing the defect energy, i.e., to minimize the number of broken atomic bonds, was earlier proposed by Tan.[26] The very small distortion of about $0.02 \pm 0.01$ nm for the {113} planes parallel to the defect plane as measured in Fig. 3(a) can be explained by an inward relaxation around each of the vacancy chains. A similar inward relaxation of the vacancy chain (0.026 nm) was also obtained by investigation of the vacancy chain relaxation based on a molecular mechanical force field (work in progress). Taking into account the lattice relaxation around the vacancy chain as shown in the model in Fig. 3(b) (eight-membered rings), HREM images of a single vacancy chain in a strained SiGe crystal have been simulated over a wide range of defocus and crystal thickness values as well as for various vacancy concentrations (vacancy occupation) along the chain (Fig. 4). It is found that the images are strongly dependent on the defocus value and on the vacancy concentration [Figs. 4(a) and 4(b)] but only weakly dependent on the crystal thickness for a focus value of $-25$ nm [Fig. 4(c)]. The experimental HREM image inside the eight-membered rings in Fig. 3(b) agrees well with the one simulated at a focus value of $-25$ nm [Fig. 3(c)].

Good agreement between the experimental and the simulated HREM images of the double-vacancy chain marked in our model in Fig. 3(b) by a ten-membered atomic ring was obtained by assuming that two nearest-neighbor vacancy chains in a strained lattice slightly shifted toward each other, over about 0.04 nm along the $[\bar{1}10]$ direction. We simulated HREM images of the extended {113} defect based on the unit cell marked in Fig. 3(b) by a large white rectangle. This unit cell includes single- and double-vacancy chains. One can see that the simulated and experimental images of the {113} defect presented in Figs. 3(a) and 3(c) are in satisfactory agreement. Note that inwardly relaxed vacancy chains are arranged along the compressive strain in the [110] direction in SiGe in order to relieve this strain.

The {113} defects, shown in Fig. 3, are only observed in the initial stages of point-defect clustering in the SiGe layer. At a final stage, after prolonged irradiation, most of the defects disappear [see Fig. 1(c)]. The process of the disappearance of a {113} defect of vacancy type was recently investigated in a Si layer close to the Si-$Si_3N_4$ interface.[17] It was shown that this process includes an interaction with interstitial atoms. But because of the existence of an energy barrier against recombination of interstitial atoms with the extended aggregate of vacancies, a large time is needed for the disappearance of the {113} defect during irradiation at room temperature.

We conclude that a small compressive strain ($-0.3\%$) in the SiGe alloy causes an initially observed clustering of vacancies on {113} planes during irradiation. These clusters are uniformly distributed within the SiGe layer and are able to relieve the compressive strain in the SiGe alloy due to an inwardly introduced lattice relaxation. The vacancy clusters slowly disappear upon further interaction with interstitials generated in SiGe.

### B. Moderately strained $Si_{1-x}Ge_x$ system with $x=0.13$ and $s=0.5\%$

The $Si/Si_{1-x}Ge_x/(001)Si$ heterostructures with a 0.5% misfit ($x=0.13$) reverses the point-defect clustering in and out of the SiGe layer. Immediately after starting the irradiation a nonuniform distribution of point-defect clusters is formed in the Si layers at a distance of 3–5 nm from the interface [Fig. 5(a)]. These clusters disappear very fast and after about 10 minutes extended {113} defects are created along the interface [Fig. 5(b)]. An enlarged HREM image of one of these defects is inserted in Fig. 5(b). It is similar to the ones presented in Fig. 3. Using the same imaging code one can conclude that the defect is of the vacancy type and consists of vacancy chains located on {113} planes. Very few {113} defects of vacancy type are formed inside the SiGe layer even after prolonged irradiation until a highly disturbed structure is formed in the rest of the SiGe layer. A new position of the interface and large roughness is now visualized, due to the formation of the disturbed structure in the SiGe layer at this stage. From Figs. 5(b) and 5(c) it is clearly seen that the position of the interface corresponding to the initial (higher) concentration of Ge atoms is shifted by over 10 nm relative to the defect *B* initially located inside the SiGe layer. No new vacancy type extended {113} defects form in the intermixed area. At the same time in the Si lay-

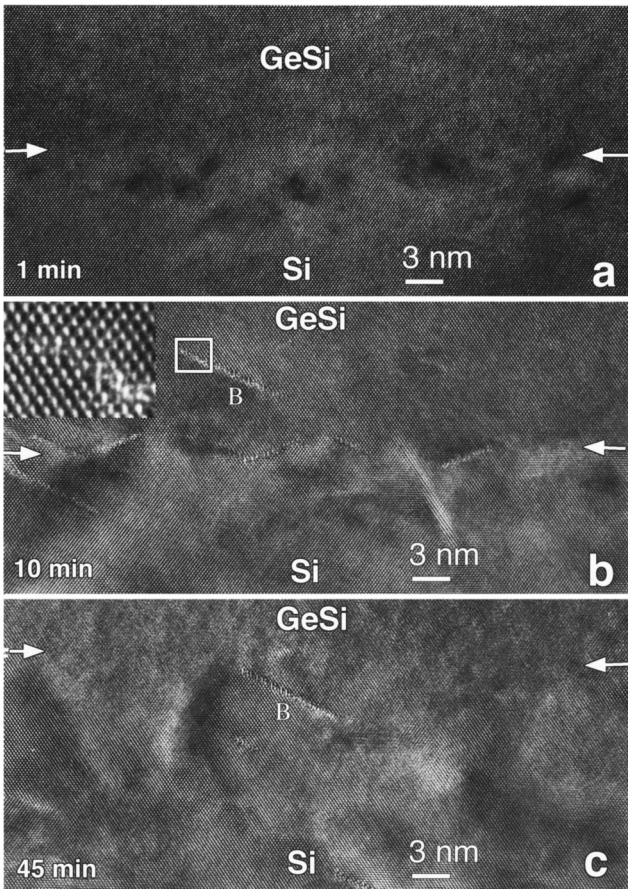


FIG. 5. HREM images of point-defect clusters formed in a strained SiGe/Si heterostructure with a 0.5% misfit at various stages of irradiation: (a) after 1 min; (b) after 10 min; (c) after 45 min. The inset in (b) corresponds to the part of the defect shown by the white rectangle.

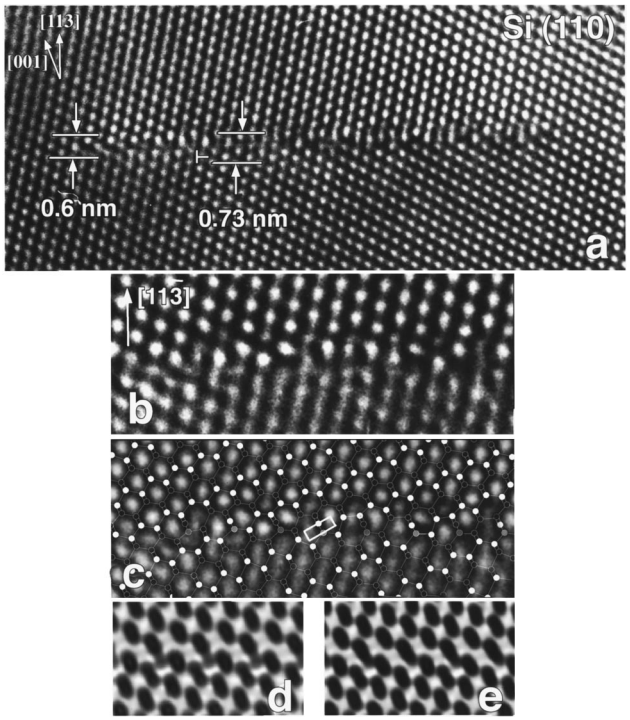


FIG. 6. (a) HREM image of a {113} defect in the Si layer, 35 nm away from the interface after 40 min of irradiation. (b) An enlarged image of the {113} defect. (c) An atomic model superimposed on the image of (b). A projection of the additional volume introduced by the [001] split-interstitial atom (gray atom) on the (110) plan is outlined by a white rectangle of $0.13\times0.38$ mm$^2$. (d) and (e) Simulated HREM images of the {113} defect based on the model presented in (c) for two different distances between the interstitial atoms in the row: (d) 0.235 nm and (e) 0.308 nm. Crystal thickness and focus value are 5 and $-55$ nm, respectively.

ers, at a larger distance from the interface than could be shown in Fig. 5(c), a number of well-extended defects are formed. One of them is presented in Fig. 6(a) and will now be analyzed. Its HREM image displays strongly [001] extended dark columns located on {113} planes. An atomic model of the defect, superimposed on the experimental image in Fig. 6(c) is similar to the one predicted in[24,26] and highlights the interstitial type defect consisting of split-[001] interstitial atoms. Each of the split interstitial atoms in the model corresponds to an additional row of interstitial atoms extended in the [110] direction. The displacement introduced by the row of interstitials can be found by direct measurement of the atom position in the experimental HREM image of Fig. 6(a). It is about $0.13\pm0.01$ nm in the [001] direction and approximately equals $a/4[001]$ as shown in Fig. 6(c) by the thick white lines. This displacement leads to the appearance of an additional {113} plane below the defect plane [see Fig. 6(a)]. This displacement, however, makes it difficult to locate the interstitial and matrix atoms in a single (110) habit plane; it results in a strong compression of the bonds, which reaches values up to 46%. Therefore two split atoms in the [110] interstitial row, located at the distance of the next-nearest-neighbor position ($a/2[110]$) have to move toward each other in order to form a pair of interstitial atoms in the relaxed configurations, as was first predicted in Ref. 24. The distance between these interstitial atoms along the [110] direction can be roughly determined from the best fit between the experimental and the simulated HREM images of the interstitial row. Figures 6(d) and 6(e) show the simulated images of interstitial rows for two different distances between interstitial atoms in the [110] direction: 0.235 (d) and 0.308 nm (e). This corresponds to 3% and 10% of the Si-Si bond compression between split and matrix atoms seen in the (110) plan view in Fig. 6(b). The best agreement between simulated and experimental images has been obtained for the larger bond compression.

We initially conclude that a compressive strain of about $-0.5\%$ suppresses the point-defect clustering in SiGe but leads to the formation of nonuniformly distributed point-defect clusters in metastable configurations at the interface and in the Si layer.

Additionally, we irradiated a relaxed $Si_{1-x}Ge_x/(001)Si$ heterostructure with $x=0.12$ at 1 MeV in a high-voltage electron microscope at temperatures between 20 and 560 °C. A high density of {113} defects is created, in thick SiGe samples over the whole temperature range and there is no cluster formation in SiGe for thicknesses less than 30–50 nm. Therefore a relaxed GeSi alloy is not expected to be informative for a HREM irradiation experiment where very thin areas (thickness below 30 nm) are used. The formation of defect clusters in thick SiGe samples clearly evidences the possibility of Frenkel pair generation in a relaxed SiGe alloy

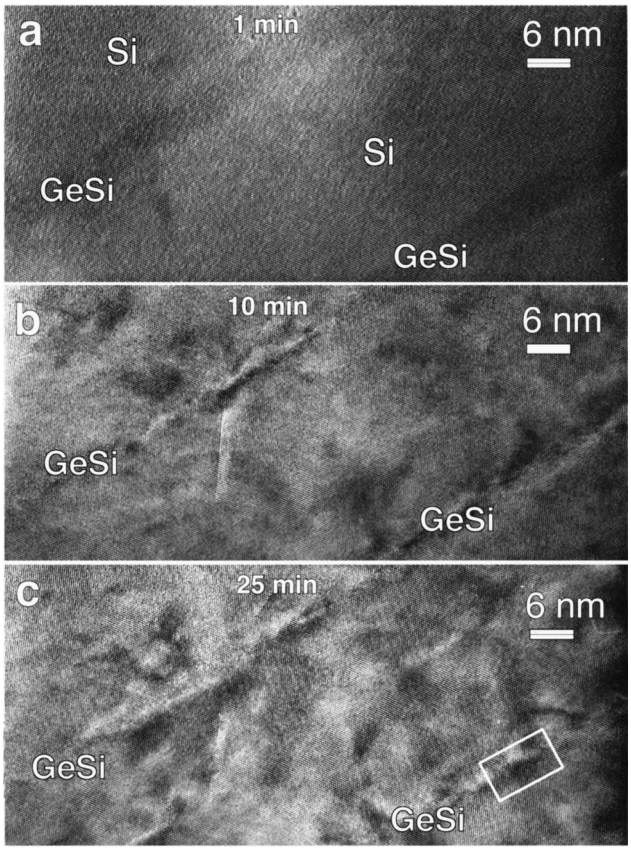


FIG. 7. Successive transformation stages of thin strained SiGe layers with a 0.9% misfit during electron irradiation at room temperature. (a) After 1 min; (b) after 10 min; (c) after 25 min.

during irradiation with 1 MeV electrons. This agrees well with the observation of {113} defect formation in alloyed Ge with 2% Si during HVEM irradiation.[13] A reduction of the Frenkel pair generation with increasing $x$ upon 400 keV irradiation would exclusively influence the nucleation time and the growth rate of the point-defect clusters in the SiGe layer but should not alter the diffusion of vacancies from the Si layer and the formation of a nonuniform distribution of vacancy-type clusters along the interface [Fig. 5(b)], which is mediated by the compressive strain in the SiGe only. We assume that the Frenkel pair separation is rather weakly dependent on the composition but strongly dependent on the compressive strain in layered SiGe.

### C. Highly strained $Si_{1-x}Ge_x$ system with $x=0.22$ and $s=0.9\%$

To reinforce the effect of intermixing we irradiated a coherently strained five-period MQW $(Si/Si_{1-x}Ge_x)_5/(001)Si$ structure with a SiGe layer thickness of 3–6 nm and a misfit up to 0.9% ($x=0.22$). Irradiation leads to a fast intermixing of the thin and initially continuous SiGe layers and partly to the formation of strongly deformed areas at the position of the strained layers [Figs. 7(a)–7(c)]. Figure 8(a) shows a typical HREM image of the deformed area. A very complex vacancy-type extended defect, lying on the (001) plane parallel to the interface, is formed. Several steps in the defect plane [look along the arrow parallel to the interface in Fig. 8(a)] and extra {111} planes located close to the steps are present in this area. Figure 8(b) shows a high magnification

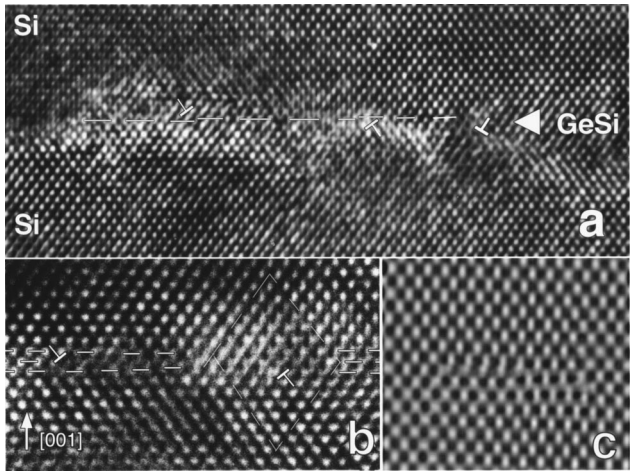


FIG. 8. Enlarged HREM image of a deformed area created in the strained SiGe layer with an initial misfit of 0.9% after 35 min of irradiation. The white broken line indicates the steps on the plane of the (001) defect (observe along the arrow). (b) HREM image of an intrinsic dislocation dipole on the (001) plane with a Burgers contour drawn around the right core of the dislocation. (c) Simulated HREM image of a 60° dislocation dipole obtained by the combination of the two models presented in Figs. 9(d) and 9(e) below.

of a small planar (001) defect [inside the white rectangle in Fig. 7(c)]. This defect highlights features of an intrinsic dislocation dipole with a (001) habit plane, since two extra {111} planes are inserted in opposite directions at the edges of the defect. The small distortion of the (001) planes parallel to the defect plane, typical for a vacancy type, is indicated in Fig. 8(b) by dashed lines. An atomic model of these (001) defects cannot be deduced from HREM images due to their complexity, but the Burgers contour drawn around the right core of the dislocation dipole in Fig. 8(b) corresponds to a perfect 60° dislocation. From simple geometrical modeling of a vacancy cluster on the (001) plane in Figs. 9(a) and 9(b), we can deduce that atoms above and below the defect plane cannot be bonded without additional cooperative atom displacements along two orthogonal directions $[\bar{1}10]$ and $[110]$ within the defect plane. Depending on the agglomeration of vacancies in a double [Fig. 9(a)] or a single [Fig. 9(b)] (001) plane, the initial displacement vector of the defect may be assumed to be $a/2[001]$ or $a/4[001]$. Figure 9(c) shows the formation of the dislocation dipole at an intermediate stage after an additional displacement along the $[\bar{1}10]$ direction: $a/2[001]+a/4[\bar{1}10]=a/4[\bar{1}\bar{1}2]$. This defect is not stable and transforms by a displacement in the orthogonal $[110]$ direction ($a/4[\bar{1}\bar{1}2]+a/4[110]=a/2[011]$) into a 60° dislocation dipole presented in Fig. 9(e). Further glide motion of one of the dislocation cores on the {111} planes should lead to the formation of a step on the defect plane and to relaxation of the strongly deformed crystal structure close to the core of the dislocation. A more complex structure of the (001) defect is formed at an intermediate stage during the aggregation of vacancies on a single (001) plane. In this case two consequent displacements on the defect plane lead to the formation of the defects: $a/4[001]+a/4[\bar{1}10]=a/4[\bar{1}11]$ and $a/4[\bar{1}11]+a/4[110]=a/4[021]$. The second one, presented in Fig. 9(d), is more stable compared to the disloca-

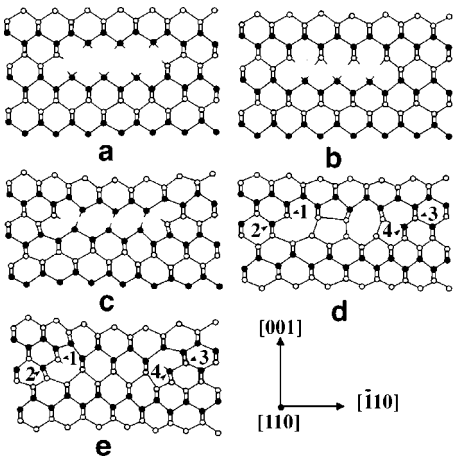


FIG. 9. (a) and (b) Vacancies located on a (001) habit plane within a double (a) and a single (b) (001) plane. (c) and (d) Intermediate stages of a dislocation dipole formation depending on the initial position of the vacancies in a double (c) or a single (d) (001) layer after an additional displacement in the defect plane (see text). (e) The final stage of a 60° dislocation dipole formation on the (001) habit plane. Atoms 1,2, and 3,4 are separated by a vertical distance of $a/4[110]$, indicative of the screw-type nature of this configuration formed by a displacement along the [110] direction.

tion dipole at the intermediate stage of Fig. 9(c). A similar structure was recently found by HREM investigations of Si-implanted crystals and predicted by molecular dynamics studies of (001) Si wafers bonding.[27,28] However, this type of defect is metastable and has to transform to a stable one. This process can be considered as a consequent structure rearrangement by interaction with additional vacancies moving to the defect plane, $a/4[021]+a/4[001]=a/2[011]$, which should again lead to the formation of a 60° dislocation dipole. Using the models presented in Fig. 9 we simulated HREM images of the dislocation dipole. The best agreement between simulated and experimental images [see Fig. 8(b) and 8(c)] has been obtained by using the model shown in Fig. 9(d), and by assuming that the right core of the dislocation dipole is rearranged into a 60° dislocation as shown in Fig. 9(e). Note that the formation of the dislocation dipole presented in Fig. 8(b) is due to irradiation of a very thin specimen. In a thicker specimen intrinsic 60° dislocation loops have to be formed. But in a very thin specimen those parts of the dislocation loop that are parallel to the sample surface can climb to the surface and create steps there.

We conclude that the irradiation of highly (0.9%) strained multilayered Si/SiGe/Si/(001)Si structures with a 3–6 nm SiGe layer thickness leads to the clustering of vacancies on the (001) plane at the position of the SiGe layers. Vacancy platelets on (001) can be relaxed by the formation of an intrinsic 60° dislocation loop. The mechanism of dislocation loop formation includes the aggregation of vacancies from a single to a double (001) and the formation of a metastable defect at intermediate stages.

## IV. DISCUSSION

### A. Chainlike clusters of point defects

Our results indicate that in weakly strained Si/SiGe/Si heterostructures (0.3–0.5 %) vacancies and interstitials produced by electron irradiation tend to aggregate in [110] chainlike configurations. These configurations are located on {113} habit planes and are characterized by a different magnitude and opposite type of lattice relaxation. The possibility of chain structure formation of both point defects in Si was predicted earlier, but without any consideration of strain or lattice relaxation introduced by the chains.[24,26,29,30] Using these chain configurations of point defects as a starting point, energetically favorable atomic models have been proposed by Tan for further homogeneous nucleation of dislocations in Si.[26] The {113} plane was predicted to be favorable for aggregation of interstitials only. However, further detailed HREM studies of the {113} defect revealed a more complex structure than the one predicted by Tan. Hexagonally arranged atomic rings followed by eight-membered rings in an irregular succession in the plane of the {113} defect produced by electron irradiation at 450 °C were first revealed by Takeda.[31] Furthermore, at room temperature both interstitials and vacancies cluster on a {113} plane if their diffusion to the surface is blocked by covering films.[14–17] According to these results the aggregation of point defects on {113} in Si layers close to the Si-$Si_3N_4$ interface can be considered rather as an additional way of point-defect recombination in an extended form in the presence of a high concentration of both types of point defects. At the initial stage, vacancies cluster in the form of [110] chains located on {113} and further act as traps for interstitials. The possibility of low-energy configuration formation of interstitial atoms inside the vacancy cluster prevents the fast recombination of point defects in extended shape.[17]

### B. Point-defect clustering in low- and moderately strained SiGe/Si systems

The model of point-defect behavior in the Si layer close to the Si-$Si_3N_4$ interface presented in Ref. 17 is in good agreement with our experimental results presented here. Indeed, vacancies generated in the strained SiGe alloy with $-0.3\%$ strain are initially precipitated as chain configurations located in the {113} planes. After about 30 minutes of irradiation these defects disappear via a similar way. Because of the very thin cross-section specimens used in the HREM experiments, this fact shows that the diffusion of both types of point defects to the surface of a strained SiGe layer is strongly decreased and the recombination of point defects inside SiGe becomes dominant. In addition, it is observed that a further increase of the compressive strain in SiGe to $-0.5\%$ suppresses cluster formation in the alloy [Fig. 5(b)]. To understand this phenomenon, we have to consider the formation volume of a Frenkel pair ($V_F^f$), which is determined by the sum of the relaxation volumes of a single interstitial atom ($V_I^{\mathrm{rel}}$) and a vacancy ($V_V^{\mathrm{rel}}$). $V_I^{\mathrm{rel}}$ can be deduced from HREM images of a row of interstitials located on a {113} plane [Fig. 6(b)]. As discussed in the previous section, the strained interstitial row along the [110] direction can be roughly considered as a succession of interstitial atoms at a distance close to $a/2[110]=0.38$ nm (or double interstitials translated with a distance of $a[110]=0.76$ nm in the relaxed interstitial row).

More important is the lattice relaxation observed around an interstitial row in a (110) cross section. In this projection

(along the interstitial row) only a single interstitial atom position is observed, which introduces a displacement of $a/4\langle 100\rangle$ ($0.13\pm0.01$ nm) to the surroundings. Because of the strong anisotropy of this displacement, the corresponding $V_I^{\mathrm{rel}}$ can be approximated as the additional volume of the box [marked in projection by a white line in Fig. 6(b)]: $V_I^{\mathrm{rel}} = 0.13\times0.38\times0.38 = 0.0188\ \mathrm{nm}^3 = 0.94\Omega$, where $\Omega = 0.020\ \mathrm{nm}^3$ is the atomic volume per silicon atom at the equilibrium density. The magnitude can be considered as a lower limit of $V_I^{\mathrm{rel}}$. It is clear that the relaxation volume for double interstitials will be twice that value: $0.13\times0.38\times0.76 = 0.0376$. This corresponds to the same value of $V_I^{\mathrm{rel}}$, which is very close to the one ($0.90\Omega$) calculated by tight-binding molecular dynamics reported in Ref. 11. Unfortunately, $V_V^{\mathrm{rel}}$ cannot be determined correctly from HREM images of a vacancy chain because this is imaged as two close-bonded vacancies (a divacancy) in a (110) cross-section. However, the small vacancy chain relaxation of about $0.02\pm0.01$ nm suggests the $V_V^{\mathrm{rel}}$ should not be as large as $V_I^{\mathrm{rel}}$ (with opposite sign) as predicted by the tight-binding molecular dynamic studies.[11] If this were true, the relaxation volumes of a vacancy and an interstitial atom would really ''cancel each other,'' and hence Frenkel pairs should be separated independently of the magnitude of compressive strain in SiGe. In this case, clustering of point defects in the bulk of a strained SiGe layer would appear to be also independent of the amount of compressive strain. However, we find that clustering of point defects in the bulk of the SiGe layer takes place only at a strain not exceeding $-0.3\%$ (Fig. 1). In a SiGe alloy with $-0.5\%$ strain [Fig. 4(b)], clustering of point defects is strongly suppressed for a long time of irradiation.

As recently found from first principles using a cluster method, the relaxation of a single vacancy depends on the state of the charge as well as on the cluster size during calculation.[12] A maximum magnitude of inwardly introduced relaxation of 0.033 nm is reached for a neutral vacancy, which corresponds to $V_V^{\mathrm{rel}} = -0.5\Omega$. Using this value we obtain $V_F^f = 0.94\Omega + (-0.5\Omega) = 0.44\Omega$. A large $V_F^f$ strongly suggests a small possibility of Frenkel pair separation in the bulk of SiGe upon increasing compressive strain. However, near the surface, Frenkel pairs can be separated by the disappearance of the interstitial atom to the surface. As a result the formation of a very disturbed structure in a narrow layer close to the surface of the SiGe can be realized after prolonged irradiation [Fig. 5(c)]. This process provides a rather small contribution to the relaxation of the SiGe layer during irradiation. In the beginning, Frenkel pairs can easily be separated in the Si layers where tensile strain relieves their separation. Nonuniform distributions of point-defect clusters near the SiGe/Si interface, shown in Figs. 5(a) and 5(b), evidence that Frenkel pairs are separated in the Si layer by the strain field of the interface and by vacancy diffusion to the compressively-strained SiGe alloy. The high supersaturation of vacancies in this area leads to clustering of vacancies in the form of chains located on {113} at the interface, as observed in Fig. 5(b). Vacancy clusters would relieve the compressive strain in SiGe due to their inwardly induced relaxation if they had not disappeared by recombination with interstitials. This fact shows the possibility of local strain relaxation via a metastable configuration of point defects after their diffusion, finally leading to an intermixing at Si/SiGe interfaces without stable defect formation.

Interstitial atoms in the Si layer create compressively strained [110] interstitial rows which are located on {113} at some distance from the interface. This configuration is not stable and has to disappear in the area of vacancy supersaturation close to the interface. The behavior of the interstitial-type {113} defect during irradiation in a HVEM was investigated in great detail in Ref. 13. It was concluded that the interaction coefficient of mobile vacancies with the metastable interstitial-type cluster is always much larger than that for the interaction of mobile interstitial atoms with an interstitial cluster. In addition, there is no detectable energy barrier for the interaction of mobile vacancies with the metastable interstitial-type cluster. For this reason we assume that small clusters of point defects created by irradiation in the Si layer in the very initial stage, 3–5 nm distance from the interface, are of interstitial type [Fig. 5(a)]. They disappear quickly upon further diffusion of vacancies from the Si layer to the SiGe/Si interface where {113} defects of vacancy type are formed [Fig. 5(b)]. The area of vacancy supersaturation in the Si layer is changed during irradiation and {113} defects of interstitial type form and disappear again. These defects become stable at a large distance from the interface in the area of interstitial supersaturation, caused by the stable sink of vacancies at the surface of the Si layer.

### C. Point-defect interaction with the surface

The surfaces of the thin samples used for HREM can act as efficient sinks for point defects. But large differences between surface arrival rates for vacancies and interstitials introduced by low-energy ion implantation are observed even for an atomically clean Si(111)$7\times7$ surface.[32] Vacancies arrive at the surface at the temperature range between 20 and 350 °C; interstitials reach the surface at temperatures around 500 °C.

It has been shown that the distance of the point-defect sink from the Si surface during electron irradiation strongly depends on the thickness of the covering film, on the rate of point-defect recombination in the bulk, and on the type and concentration of the doping atoms.[13,14] To decide whether the reaction kinetics of the point defects are dominated by the free surface or by the recombination rate of point defects in the bulk we have to consider the quasi-steady-states during irradiation, where the defect clusters grow at a constant rate. At $T>350$ °C and for irradiation intensities $I<6\times10^{18}$ electrons/cm$^2$ s, a very long quasistationary growth of interstitial type {113} defects in *p*-type Si was found.[14] This growth is governed by an infinitely strong sink of vacancies at the surface, and the kinetic growth of {113} defects can be considered as dominated by the free surface because the defect growth rate is proportional to the rate of point-defect generation, which is proportional to *I*. An increase of the recombination rate of point defects in bulk Si for $I>6\times10^{18}$ electrons/cm$^2$ s decreases the probability of point-defect arrival at the surface and the kinetic growth of {113} defects becomes proportional to the square root of the point-defect generation rate.[13,14]

A much more complex behavior of point defects in pure Si is realized by a HVEM irradiation at room

temperature.[14,17] There is not any quasi-steady-state in this case and a recombination of point defects into extended defects is observed. It is unclear in this case whether the reaction kinetics of the point defects is dominated by the recombination of point defects or by the free surface. Some of the vacancies reach the surface because an interstitial supersaturation is established by electron irradiation of samples with thickness above 10 nm, and vacancy clusters transform into interstitial clusters.[17] However, we have never observed a similar effect in strained SiGe layers; only the disappearance of the vacancy clusters was observed [Figs. 1(a)–1(c)]. We therefore assume that the recombination of point defects dominates in a strained SiGe layer.

The large difference between $V_V^{\mathrm{rel}}$ and $V_I^{\mathrm{rel}}$ allows an explanation of the difference between the interaction coefficients of point defects with the surface, previously found in nonstrained Si and Ge crystals.[13] Weakly relaxed vacancies always tend to diffuse to the surface of a nonstrained crystal because the interaction of surface atoms with vacancies prevents an increase of the crystal volume. Once generated, interstitial atoms always increase the volume of the crystal, independent of their location in the bulk or at the surface of the crystal. In our case an additional limitation occurs for the diffusion of interstitials to the surface of the SiGe layer under compressive strain in the [110] direction. Limited diffusion of interstitials to the surface and the necessary aggregation of vacancies in the strained SiGe give rise to a recombination of point defects through an extended form in the alloy, even at a low compressive strain. Since the possibility of Frenkel pair separation in SiGe is also decreased by increasing the compressive strain, there is only one way for the strained SiGe layer to relax during irradiation: a diffusion of vacancies from the Si layers leading to an intermixing at the SiGe/Si interfaces.

### D. Point-defect clustering in a highly strained system

The results obtained show that the mechanism of vacancy clustering at the SiGe/Si interface strongly depends on the magnitude of strain in SiGe. At low strains ($-0.3\%$ to $-0.5\%$) vacancies aggregate in the form of metastable [110]-oriented chains, located on {113} planes. Assuming the crystal thickness to be 6.2 nm and the vacancy occupation along the chain to be 0.5–1.0, each of the {113} defects of vacancy type contains about $(0.8–2)\times10^2$ vacancies. Considering the density of defects in Fig. 5(b) the concentration of vacancies clustered in {113} defects is about $(3–8)\times10^{20}$ cm$^{-3}$. From Figs. 5(b) and 5(c), it is clearly seen that these defects disappear during prolonged irradiation. As discussed above, this corresponds to the relaxation of the strained SiGe layer via diffusion of vacancies leading to intermixing at the SiGe/Si interfaces without stable defect formation. Strain of about $-0.9\%$ dramatically changes the mechanism of vacancy clustering at the interface, so that the formation of intrinsic $60°$ dislocation dipoles become possible. Assuming the same crystal thickness and the density of dislocation dipoles at the interface to be about $4\times10^{12}$ cm$^{-2}$ [Fig. 8(a)], as well as the number of vacancies per single dipole of about $(2–3)\times10^2$, the concentration of vacancies clustered into dipoles is about $(1–2)\times10^{21}$ cm$^{-3}$. This means that dislocation dipole formation on a (001) plane needs a higher concentration of vacancies. However, higher vacancy supersaturation close to the interface in this case is not the single reason for preferential aggregation of vacancies on (001). Biaxial strains seem to influence the clustering of vacancies at an increased misfit due to a higher mobility of the vacancies along the compressive strain parallel to the interface compared to the [001] direction for the tensile strain.[10] If the mobility of vacancies in the highly strained GeSi layer had been isotropic, clustering of vacancies on the other habit planes ({113}) would occur, as, for instance, in low-strained SiGe. It is clear that the formation of $60°$ dislocation dipoles at the interface allows the strains in the SiGe layer to relax more effectively and to prevent further intermixing at the SiGe/Si interface during irradiation. We assume that some of the strongly deformed areas shown in Figs. 8(b) and 8(c) are the islands of the SiGe alloy relaxed by clustering of vacancies on (001).

The geometrical model of vacancy clustering on (001) presented in Fig. 9 proposes some different mechanism of the intrinsic $60°$ dislocation loop formation at the interface of a strained system. The mechanism includes the aggregation of vacancies on a double (001) plane to be accomplished by the formation of a metastable defect at intermediate stages. This model differs from the ones presented in Ref. 26, which were based on gliding of a single vacancy chain in various habit planes. We could not find in our experiments the transformation of a single vacancy chain into a dislocation dipole even after long irradiation times [Figs. 1(a)–1(c)] but its recombination with interstitials. Only clustering of vacancies in the (001) plane leads to the formation of dislocation dipole. The problem of atom bonding in the plane of the vacancy cluster in (001) is similar to that for (001)Si surfaces brought into contact. Unavoidable rotational misorientation between the bonded (001)Si wafers introduces bond distortions which relax to form a square grid of $a/2\langle110\rangle$ screw dislocations.[33] Clustering of vacancies on (001) introduces a prismatic bond distortion in the [001] direction perpendicular to the interface, which relaxes by the formation of $60°$ dislocation loops. It is believed that this mechanism can also be realized during the growth of a highly strained system due to preferential point-defect generation near the interface. In any case, our model of a $60°$ dislocation formation including clustering of vacancies on (001) is able to explain the reported high density of dislocations during enhanced Ge-Si interdiffusion.[1]

## V. CONCLUSION

*In situ* HREM irradiation of strained Si/SiGe/Si(001)Si structures is a powerful method for the investigation of point-defect behavior. We present an experimental attempt to determine the relaxation volume of an interstitial atom from HREM observations of the [110] rows of interstitials located on {113} planes. Important information concerning the lattice relaxation around a vacancy is also obtained from the HREM image of chainlike configurations of vacancies. The very small inward relaxation of the vacancy chains allows us to obtain a more accurate magnitude for the relaxation volume of a single vacancy. Based upon these results a large formation volume of the separated Frenkel pair ($V_F^f$) is proposed in Si (within $0.44\Omega$). These experimental findings enable us

to propose some insight into the process of point defect clustering in a strained system and into the mechanism of point-defect interaction with the surface. A strongly limited sink of both point defects to the SiGe surface as well as the large magnitude of $V_F^f$ give rise to an enhanced recombination of point defects in the compressive-strained SiGe during irradiation, so that relaxation is mediated by vacancies diffusing from the Si layers. The concentration of vacancies close to the SiGe/Si interface and the mechanism of vacancy clustering are governed by the initial magnitude of the biaxial strain in SiGe. Low strains ($-0.3\%$ to $-0.5\%$) induce the formation of metastable chainlike configurations of vacancies, which corresponds to a diffusive intermixing at the interface without stable defect formation. A biaxial strain corresponding to a 0.9% misfit induces a very large supersaturation of vacancies close to the interface and preferential aggregation of vacancies on the (001) plane which relaxes to form stable intrinsic 60° dislocation loops.

## ACKNOWLEDGMENTS

This work was sponsored by the Russian Foundation of Basic Research (RFBR) Grant No. 98-02-17798. The work was performed within the framework of the IUAP 4/10 project. The authors are indebted to Professor S. Amelinckx for helpful discussions. One of the authors (O.A.M.) wishes to acknowledge the UK Royal Society for funding his visit to Warwick University and Dr. C. P. Parry and Dr. N. P. Barradas for fruitful discussions.

*Present address: Institute of Semiconductor Physics RAS, pr. Lavrentjeva 13, 630090 Novosibirsk, Russia.

†On leave from Institute of Crystallography RAS, Leninsky pr. 59, 117333 Moscow, Russia.

‡Author to whom correspondence should be addressed.

§On leave from Institute of Radiophysics and Electronics NAS of Ukraine, ul. Ac. Proscura 12, Kharkov 310085, Ukraine.

[1] S. S. Iyer and F. K. LeGoues, J. Appl. Phys. **65**, 4693 (1989).

[2] J. W. Cahn and J. E. Hilliard, J. Chem. Phys. **28**, 258 (1958); J. W. Cahn, Acta Metall. **9**, 795 (1961).

[3] N. Moriya *et al.*, Phys. Rev. Lett. **71**, 883 (1993).

[4] F. H. Baumann *et al.*, Phys. Rev. Lett. **73**, 448 (1994).

[5] N. E. B. Cowern *et al.*, Phys. Rev. Lett. **72**, 2585 (1994).

[6] P. Kuo *et al.*, Appl. Phys. Lett. **62**, 612 (1993).

[7] P. Kuo *et al.*, Appl. Phys. Lett. **66**, 580 (1995).

[8] P. Kringhoj, A. Nylandsted-Larsen, and S. Y. Shirayev, Phys. Rev. Lett. **76**, 3372 (1996).

[9] A. Antonnelli and J. Bernholc, Phys. Rev. B **40**, 10 643 (1989).

[10] N. J. Aziz, Appl. Phys. Lett. **70**, 2810 (1997).

[11] N. Tang *et al.*, Phys. Rev. B **55**, 14 279 (1997).

[12] S. Ogut, H. Kim, and J. R. Chelikowsky, Phys. Rev. B **56**, 11 353 (1997).

[13] A. L. Aseev, L. I. Fedina, D. Hoehl, and H. Barsch, *Clusters of Interstitial Atoms In Silicon and Germanium* (Akademie-Verlag, Berlin, 1994), p. 152.

[14] L. Fedina, A. Gutakovskii, A. Aseev, J. Van Landuyt, and J. Vanhellemont, in *Intrinsic Point Defect Clustering in Si: A Study by HVEM and HREM in situ Electron Irradiation*, edited by Pratibha L. Gai (Kluwer, Dordrecht, 1997), p. 63.

[15] L. Fedina *et al.*, Philos. Mag. A **77**, 423 (1998).

[16] L. Fedina *et al.*, in *Microscopy of Semiconducting Materials 1997*, edited by A. G. Cullis and J. L. Hutchison, IOP Conf. Proc. No. 157 (Institute of Physics, London, 1997), p. 55.

[17] L. Fedina *et al.*, Phys. Status Solidi B **171**, 147 (1999).

[18] L. Fedina *et al.*, *Microscopy of Semiconducting Materials 1997* (Ref. 16), p. 55.

[19] T. E. Whall *et al.*, Appl. Phys. Lett. **64**, 357 (1994).

[20] V. I. Khizhny *et al.*, Appl. Phys. Lett. **69**, 960 (1996).

[21] O. A. Mironov *et al.*, Thin Solid Films **306**, 307 (1997).

[22] N. P. Barradas *et al.*, Phys. Rev. B **59**, 5097 (1999).

[23] V. I. Vdovin *et al.*, Crystallogr. Rep. (to be published).

[24] J. Corbett and J. Bourgoin, in *Point Defect in Solids*, edited by J. H. Crawford and L. N. Slifkin (Plenum, New York, 1975), Vol. 2.

[25] S. Takeda and S. Horiuchi, Ultramicroscopy **56**, 144 (1994).

[26] T. Y. Tan, Philos. Mag. A **44**, 101 (1981).

[27] S. Muto and S. Takeda, Philos. Mag. Lett. **72**, 99 (1995).

[28] A. Y. Belov, D. Conrad, K. Scheerschnidt, and U. Gosele, Philos. Mag. A **77**, 55 (1998).

[29] W. Krakow, T. Y. Tan, and H. Foll, in *Microscopy of Semiconducting Materials 1981*, edited by A. G. Cullis and D. C. Joy, IOP Conf. Proc. No. 60 (Institute of Physics, London, 1981), p. 23.

[30] J. Friedel, *Radiation Effects on Semiconductors* (Journee d'Electronique, Toulouse, 1967), Vol. I, Paper A-11.

[31] S. Takeda, N. Kohyama, and K. Ibe, Philos. Mag. A **4**, 287 (1994).

[32] P. J. Bedrossian, M.-J. Caturla, and T. Diaz de la Rubia, Appl. Phys. Lett. **70**, 176 (1997).

[33] A. Plossl and G. Krauter, Mater. Sci. Eng., R. **25**, 1 (1999).